HHS Public Access

Author manuscript

Mol Cell. Author manuscript; available in PMC 2017 July 21.

Published in final edited form as:

Mol Cell. 2016 July 21; 63(2): 240–248. doi:10.1016/j.molcel.2016.05.040.

Redox Nanodomains are Induced by and Control Calcium Signaling at the ER-mitochondrial Interface

David M. Booth[1], **Balázs Enyedi**[2], **Miklós Geiszt**[2], **Péter Várnai**[2], and **György Hajnóczky**[1]

[1]MitoCare Center, Department of Pathology, Anatomy and Cell Biology, Thomas Jefferson University, Philadelphia, PA

[2]Department of Physiology, Semmelweis University, Faculty of Medicine, H-1444 Budapest, Hungary

Abstract

The ER-mitochondrial interface is central to calcium signaling, organellar dynamics and lipid biosynthesis. The ER and mitochondrial membranes also host sources and targets of reactive oxygen species (ROS) but their local dynamics and relevance remained elusive since measurement and perturbation of ROS at the organellar interface has proven difficult. Employing drug-inducible synthetic ER-mitochondrial linkers, we overcame this problem and demonstrate that the ER-mitochondrial interface hosts a nanodomain of H_2O_2, which is induced by cytoplasmic [Ca^{2+}] spikes and exert a positive feedback on calcium oscillations. H_2O_2 nanodomains originate from the mitochondrial cristae, which are compressed upon calcium signal propagation to the mitochondria, likely due to Ca^{2+}-induced K^+ and concomitant water influx to the matrix. Thus, ER-mitochondrial H_2O_2 nanodomains represent a novel component of inter-organelle communication, regulating calcium signaling and mitochondrial activities.

Graphical Abstract

Correspondence to: Dr. György Hajnóczky, MitoCare Center, Department of Pathology, Anatomy and Cell Biology, Suite 527 JAH, Thomas Jefferson University, Philadelphia PA 19107, USA, Tel. (215) 503-1427, Fax. (215) 923-2218, gyorgy.hajnoczky@jefferson.edu.

Author Contributions

Conceived and designed the experiments: D.B., and G.H.
Created new reagents: P.V., B.E., M.G.
Executed and analyzed the experiments: D.B.
Wrote the manuscript: D.B. and G.H.

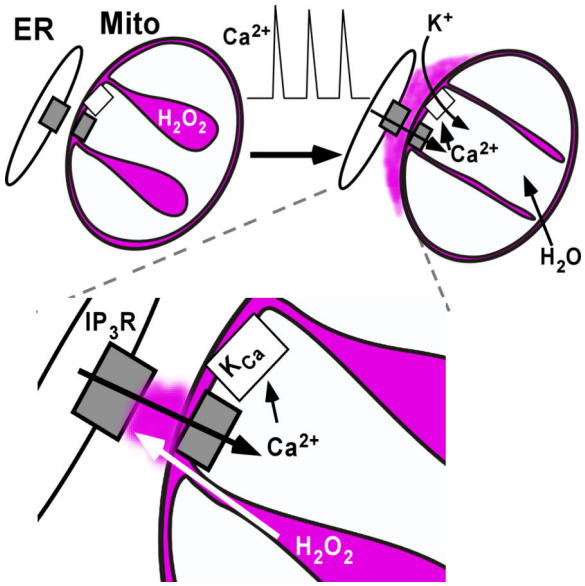

Introduction

The endoplasmic reticulum (ER) and mitochondria are tethered by robust physical linkages (Csordas et al., 2006), creating a nanometer-scale volume where sources of reactive oxygen species (ROS) and Ca^{2+} are gathered, supporting the formation of high Ca^{2+} microdomains during Ca^{2+} release events from channels residing in the ER membrane (Csordas et al., 2010; Giacomello et al., 2010; Rizzuto et al., 1993). Mitochondria require such microdomains to effectively uptake Ca^{2+} via the uniporter (Csordas et al., 1999; Kirichok et al., 2004; Rizzuto et al., 1998). Mitochondrial Ca^{2+} uptake controls both physiological and pathological processes, including aerobic metabolism (Duchen, 1992; Jouaville et al., 1999) and apoptosis (Szalai et al., 1999).

During ATP production, the electron transport chain (ETC) leaks electrons from complexes I/III forming ROS in the intermembrane space (IMS) where the oxidizing environment facilitates protein folding (Bader et al., 1999). Mitochondria-derived ROS were also measured in the cytoplasm and have been linked to both physiological and pathological mechanisms (Aon et al., 2003; Sena and Chandel, 2012; Umanskaya et al., 2014; Zorov et al., 2000). Like mitochondria, the ER hosts ROS production mechanisms which drive oxidative protein folding in the ER lumen (Araki et al., 2013) and cytoplasmic signaling pathways (Li et al., 2009). ROS are known to modulate ER Ca^{2+} transport mechanisms (Bansaghi et al., 2014; Bootman et al., 1992; Csordas and Hajnoczky, 2009; Prosser et al., 2011) but the role of mitochondrial or ER-derived ROS in local Ca^{2+} signaling remains elusive. A major reason for this is that measurement and manipulation of ROS at the close quarters of the ER-mitochondrial interface has been difficult.

Results

To overcome this problem, we used drug-inducible synthetic linkers to target fluorescent H_2O_2 sensors and ROS producers to the close associations of ER and mitochondria. This

strategy is based on drug-inducible linkers that we have recently created and validated for measuring [Ca^{2+}] at the ER-mitochondrial close contacts (Csordas et al., 2010). Briefly, ER membrane (ER-M) and outer mitochondrial membrane (OMM) targeting sequences were linked to the 2 halves of the FKBP-FRB drug inducible heterodimerization system through a fluorescent protein each. The expressed constructs showed ER and mitochondrial distribution, respectively (Fig. 1A, upper). Upon addition of rapamycin the 2 linker halves became crosslinked and rapidly concentrated only at the sites where the 2 organelles are close to each other (Fig. 1A, lower). We have previously shown by FRET and ultrastructure analysis that linkers concentrate at the ER-mitochondrial interface without distorting ER morphology (Csordas et al., 2010). Here, we sought to further demonstrate the migration of the ER-M-targeted linker half molecules across the membrane surface to be trapped by OMM-targeted linker half molecules at pre-existing contact points in the presence of rapamycin. To this end, HepG2 cells were triple-transfected with ER-M-CFP-FRB, ER-lumen-GFP and OMM-RFP-FKBP and subjected to co-localization analysis by confocal microscopy (Fig. 1B&S1AB). Before rapamycin treatment, the ER-M linker half was mostly co-localized with the ER-lumen marker (Fig. 1B, cyan-green) and showed little co-localization with the OMM linker halves (cyan-red). Upon addition of rapamycin (for 4 min) the co-localization of the ER-M and ER-lumen probes decreased (Fig. 1B&S1B), whereas the co-localization between ER-M and OMM greatly increased (Fig. 1B) until rapamycin wash-out and further heterodimerization were blocked (FK506, 5 μM). There was only a relatively small increase in the co-localization between the OMM-targeted linker half and the ER-lumen marker during rapamycin treatment (Fig. 1B, green-red). Quantitative analysis of the co-localization shows that the majority of the linkers became concentrated at the ER-mitochondrial associations and both the co-localization analysis and the images indicate that the ER morphology remained essentially unchanged during the rapamycin treatment (Fig. 1B upper vs. lower row, green). Images of the whole cell corresponding to the area shown in Fig. 1B and the rapamycin-induced separation of the ER-M linker half from the bulk ER marker are displayed in Fig. S1AB.

Next, we replaced the fluorescent proteins in the linker halves with a fluorescent ROS sensor. We selected HyPer because it is a monomeric, ratiometric probe that specifically, directly and reversibly senses H_2O_2 with high temporal resolution. To simplify the interpretation of data, we made paired measurements in every location with the recommended negative control probe, SypHer (Bilan and Belousov, 2016). SypHer is identical to HyPer except for the replacement of C199 with S199 rendering the protein H_2O_2 insensitive. Since, SypHer and HyPer, both share an identical YFP fluorophore core which displays a decrease in short wavelength absorption (415 nm) and corresponding increase in long wavelength (495 nm) absorption in response to alkaline conditions owing to a deprotonation of the fluorophore core, SypHer can be used as control for pH artifacts. The images in Fig. 1C show the rapamycin induced rearrangement of the ER-M-targeted HyPer from a broad ER distribution to colocalization with the OMM marker. After validation of the proper distribution, HyPer (or SypHer) was inserted into both the ER-M and OMM linker components.

HyPer fluorescence ratio was acutely sensitive to oxidation by exogenously added H_2O_2 (200 μM) and subsequent reduction with dithiothreitol (DTT; 5 mM) (Fig. 1D). Sensitivity

to low μM concentrations of H_2O_2 was also validated in permeabilized cells (Fig. S1C). The fluorescence ratio for SypHer was similar to that for HyPer in untreated cells but did not respond to H_2O_2 or DTT addition (Fig. 1D). Thus, SypHer was confirmed as a negative control for HyPer and was included in all experiments to isolate the effects of H_2O_2. In the pairs of HyPer and SypHer experiments, elevated HyPer ratio indicated exposure of the probe to H_2O_2. When linker pairs were targeted to the interface with a pulse of rapamycin (100 nM, 3 min, FK506 wash, 5 μM) we detected moderate but significantly elevated H_2O_2 in unstimulated cells (Fig. 1E). However, when the same probes distributed along the entire membrane surfaces of the ER-M or OMM we saw no difference under resting conditions (Fig. 1E). Similarly, H_2O_2 was undetectable within the cytosol or surprisingly, the mitochondrial matrix (Fig. 1E). Notably, both HyPer and SypHer ratios were high in the mitochondrial matrix due to the alkaline pH. When targeted to the ER-lumen, HyPer was almost completely oxidized, consistent with the oxidized redox potential of the compartment (Fig. 1E) (Bilan and Belousov, 2016). Thus, these results indicated that the ER-mitochondrial interface is continuously exposed to a low level of H_2O_2.

To determine the influence of Ca^{2+} in shaping the interface redox environment, we stimulated cells with an IP_3-linked agonist and a SERCA inhibitor, thapsigargin (Tg), to elicit ER Ca^{2+} release. The Ca^{2+} release resulted in a $[Ca^{2+}]_c$ transient measured with the Ca^{2+} sensitive fluorophore fura2 (Fig. 2A upper). Parallel recordings with interface HyPer and SypHer showed an increase in the HyPer ratio and a decrease in the SypHer ratio, which indicated that the $[Ca^{2+}]_c$ elevation was accompanied by a rise in H_2O_2 (Fig. 2A). The decrease in the SypHer ratio likely reflected acidification that could result from Ca^{2+}-induced dissociation of H^+ from Ca^{2+} binding species. The H_2O_2 elevation followed the rise of the $[Ca^{2+}]_c$ signal before decreasing toward the baseline. The agonist-induced rise in H_2O_2 was detected only when Hyper was targeted to the interface by rapamycin pretreatment, whereas the acidification appeared regardless of the rapamycin pretreatment (Fig. S2A). Comparison of the interface targeted HyPer/SypHer with probes distributed uniformly across the OMM and ER surfaces (either only OMM-targeted or ER-M-targeted probe was expressed) respectively, confirmed that the H_2O_2 elevation was confined to the ER-mitochondrial interface (Fig. 2B). To test the specific contribution of the IP_3 receptors, the effect of Tg alone was also evaluated. Tg elicited a slower, less pronounced elevation of $[Ca^{2+}]_c$ consistent with ER-Ca^{2+} leak and no change in the interface H_2O_2 (Fig. 2C). We quantified the area under the curve response $HyPer/SypHer_{Stimulation}$-$HyPer/SypHer_{Baseline}$ for each condition, which confirmed that a significant H_2O_2 response occurred only at the interface and only when the IP_3 receptor-mediated Ca^{2+} release was activated (Fig. 2D; * $p = < 0.05$). Other compartments, cytosol, ER-lumen and mitochondrial matrix were without elevations upon stimulation (Fig. S2B–D). Notably, the addition of rapamycin did not alter the HyPer/SypHer responses when the probes were targeted to these compartments (Fig. S2B–D).

We next showed that interface H_2O_2 elevations could be evoked by multiple IP_3-linked agonists and independently of SERCA inhibition (Fig. 3A&B). Furthermore, we confirmed that the elevations derived from the H_2O_2-sensing thiol pair within HyPer, as demonstrated by DTT sensitivity (Fig. 3AB&D) and that the signal was mediated by H_2O_2, based on the effects of the H_2O_2 scavenger, ebselen (Fig. 3C&D).

To dissect the mechanism underlying the interface H_2O_2 elevation, we selectively removed candidate components. When the agonist-evoked $[Ca^{2+}]_c$ rise was prevented, by pre-depletion of ER Ca^{2+} using Tg, the H_2O_2 rise was not observed (Fig. 3E&H). Similarly, blockade of the ETC at two points (Fig. 3F&H), or dissipation of the inner mitochondrial membrane (IMM) potential abolished the H_2O_2 elevation (Fig. 3G&H), whereas the $[Ca^{2+}]_c$ signal was not suppressed (Fig. S3). Thus, the $[Ca^{2+}]_c$ signal and the ensuing $[Ca^{2+}]_m$ rise enables H_2O_2 of mitochondrial ETC origin to form a spatiotemporally confined elevation of H_2O_2 at the ER-mitochondrial interface.

To understand how Ca^{2+} engages mitochondrial H_2O_2, we first investigated whether the mitochondrial ultrastructure changes in response to agonist stimulation. Naive cells feature a cohort of narrow cristae and a second population of dilated (> 30 nm) cristae, indicating large intracristal volume (Fig. 4A,B left & S4A; *gray*). Following treatment with an IP_3-linked agonist ATP, we observed fewer dilated cristae (Fig. 4B right & S4A; *black*). Since mitochondrial cross-sectional area or aspect ratio were unchanged (Fig. S4B), the decrease in cristae volume was likely due to a proportional increase in matrix volume. We reasoned that the $[Ca^{2+}]_m$ increase might activate mitoK_{Ca} channels (Singh et al., 2013; Xu et al., 2002), to increase matrix volume through K^+ and parallel H_2O influx (Marchissio et al., 2012). Indeed, a mitoK_{Ca} inhibitor, paxilline, abolished the agonist-induced collapse of dilated cristae (Fig. 4C&S4A; *purple*). Similarly, when we induced movement of K^+ into the matrix with low-dose valinomycin that does not cause depolarization (Liu and Hajnoczky, 2011), large-volume cristae were also absent (Fig. 4C&S4A; *pink*). When agonist-induced changes in cristae volume were prevented by pretreatment with paxilline or low-dose valinomycin, the interface H_2O_2 transient was absent (Fig. 4D, lower). This happened despite similar $[Ca^{2+}]_c$ and $[Ca^{2+}]_m$ elevations (Fig. 4D, upper), and no change in mitochondrial membrane potential (Liu and Hajnoczky, 2011) suggesting that the agonist-induced $[Ca^{2+}]_m$ rise induces mitochondrial matrix expansion that compresses the cristae. This also indicated the possibility that the content of the cristae might be of relevance for the agonist-induced H_2O_2 rise detected at the ER-mitochondrial interface.

By targeting HyPer and SypHer to the mitochondrial intermembrane space (IMS), where it's location was confirmed using trypan blue quenching (Fig. S4D), we showed that the resting HyPer/SypHer ratio was higher than the OMM, and that DTT addition decreased the HyPer/SypHer ratio (Fig. S4D), indicating the presence of H_2O_2. HyPer/SypHer recordings revealed that agonist stimulation did not change the concentration of H_2O_2 in the IMS (Fig. S4E). Thus, concentration change of H_2O_2 at the interface likely originates from the IMS, involving a volume increase in the mitochondrial matrix and the ensuing compression of the cristae that forces the H_2O_2-rich cristae content to the OMM surface. Since matrix volume expansion might be greatest in the region of mitochondrial Ca^{2+} uptake, the $[H_2O_2]$ rise can be concentrated to the region of the Ca^{2+}-transfer represented by the ER-mitochondrial interface. Furthermore, ultrastructural analysis revealed a significant clustering of cristae openings juxtaposed to the ER-mitochondrial interface (Fig 4A, Fig. S4C, left; *gray*) compared to the frequency predicted if cristae were uniformly distributed (Fig. S4C, left; *white*). Conversely, cristae openings were not enriched in mito-mito interactions in HepG2 cells (Fig. S4C right) as reported in other cells (Picard et al., 2015).

To explore the functional consequences of the H_2O_2 nanodomain, we first, artificially produced ROS at the interface using Killer Red (KR) targeted with the ER-mitochondrial linker. Illumination at the excitation wavelength of KR sensitized cells to threshold concentrations of IP_3-linked agonist (loATP, ATP, 1 μM) as reflected in the cytoplasmic [Ca^{2+}] signal (Fig. 5A, control; *black*, illuminated; *red*). The presence of ebselen abolished this effect (Fig. 5A; *orange*). Furthermore, no sensitization was observed when KR was targeted to the nucleus, far from the ER-mitochondrial interface (Fig. 5A; *blue*). Supramaximal agonist, hiATP, (ATP, 100 μM) was used in each condition to ensure cells were capable of Ca^{2+} release (Fig. 5A). After we demonstrated the sensitivity of IP_3-induced Ca^{2+} release to artificial oxidation of the interface, we turned to the role of the H_2O_2 originating from the mitochondrial cristae. Using sensitivity to suboptimal ATP (loATP) as our assay, we observed repetitive calcium oscillations, in approximately 40% of cells (Fig. 5B, left). When compression of the cristae was prevented by inhibiting K^+ influx with paxilline only 20% of the total cells exhibited repetitive Ca^{2+} spikes (Fig. 5B, right). Furthermore, when we disrupted the ER-mitochondrial interface by relocating mitochondria close to the plasma membrane, using constitutive mitochondria-plasma membrane linkers, sensitivity of the cytoplasmic [Ca^{2+}] signal to loATP agonist fell significantly (Fig. 5C).

Discussion

Our results demonstrate the existence of a dynamic H_2O_2 nanodomain at the ER-mitochondrial interface that is induced by and influences Ca^{2+} signals (see scheme in Fig. 5D). The H_2O_2 likely originates from within the cristae where elevated H_2O_2 generated by ETC activity was measured (Fig. S4E). Since the IMS displays permanently elevated H_2O_2 as compared to the matrix or OMM surface (Fig. S4E), we think that H_2O_2 is continually produced in the IMS and its elimination by degradation and diffusion to the matrix and cytoplasm is slower than the production. During the interface [H_2O_2] rise the IMS [H_2O_2] did not change (Fig. S4F) but the IMS volume decreased (Fig. 4), thus we propose that H_2O_2 dissolved within the IMS content is forced to the ER-mitochondrial interface.

Previously, localized ROS elevations have been claimed but their origin was either extra-mitochondrial (Prosser et al., 2011) or were observed in the mitochondrial matrix isolated from and independent of Ca^{2+}-release proteins (Wang et al., 2008). We considered the possibility of a burst of *de novo* H_2O_2 generation mediated by Ca^{2+}-stimulated acceleration of ETC. However, we did not detect agonist-evoked H_2O_2 in the IMS (Fig. S4F) or matrix (Fig. S2C). Furthermore, during treatment with paxilline or low concentration valinomycin, the IP_3-linked $[Ca^{2+}]_m$ signal was maintained, and therefore the Ca^{2+}-induced increase in ETC likely occurred but the H_2O_2 nanodomain was abolished. Thus, Ca^{2+}-stimulated acceleration of ETC activity is unlikely to be the primary reason for the H_2O_2 nanodomain. Rather, our data support that mitochondrial respiration generates H_2O_2 in the IMS/cristae space, Ca^{2+} uptake induces compression of the dilated cristae to force their volume through aligned cristae junctions to the ER-mitochondrial interface, causing a transient elevation of H_2O_2 (Fig. 5D). We point out that a small % increase in the matrix volume results in a large-scale change in the cristae volume. Mechanistically, uptake of Ca^{2+} to the matrix likely stimulates mitoK_{Ca}-mediated influx of K^+ instigating rapid osmotic changes in the matrix, compensated by H_2O influx. A similar mechanism has been linked to the matrix swelling

observed in isolated mitochondria and hepatocytes (Halestrap et al., 1986; Quinlan et al., 1983). We propose that H_2O_2 generated by the ETC accumulates within the lumen of cristae, consistent with the concentration of ETC components on cristae membranes (Cogliati et al., 2013). Our data also show that the cristae openings are preferentially oriented towards the ER-mitochondrial interface (Fig. 4A&S4C) and thus, inform a model where H_2O_2-enriched cristae content is forced to the ER-mitochondrial interface upon mitochondrial Ca^{2+} and K^+ induced matrix expansion (Fig. 5D). The restricted volume of the ER-mitochondrial interface suggests limited antioxidant capacity that is overwhelmed by focused elevations of H_2O_2. We used ebselen as an enhancement to the catalytic potential of the interface redox environment. Since ebselen and glutathione share limited direct reactivity with H_2O_2, it is likely that ebselen acts to increase the catalytic rate by enhancing the reaction of H_2O_2 with the existing thioredoxin reductase and glutathione systems (Dickinson and Forman, 2002; Zhao et al., 2002). Ebselen suppressed the IP_3-linked interface HyPer signal but failed to abolish the effect of the exogenously added H_2O_2. We think that increasing the catalytic potential can be effective to counteract the agonist-induced local H_2O_2 response but it cannot suppress the exogenous H_2O_2's effect that homogenously increases H_2O_2 in the entire cellular volume.

While HyPer is H_2O_2 specific, it might be possible that the H_2O_2 increase reflects accumulation of superoxide anion. In this model, superoxide may be dismutated in the IMS or the interface itself to be detected as H_2O_2 by HyPer, however, the half-life of superoxide and cytochrome c activity in the IMS make this unlikely (Zhao et al., 2003). H_2O_2 derived from the cristae have multiple means to traverse the OMM at the ER-mitochondrial interface. Previously, IP_3 receptors have been reported to form a complex with VDAC proteins, the major pore proteins of the OMM (Szabadkai et al., 2006). Therefore, VDACs are likely to be abundant at the relevant OMM area. Also, a collection of other mitochondrial and ER proteins have been localized to the ER-mitochondrial associations, which might also facilitate the passage of H_2O_2. The lipid composition of the ER-associated mitochondrial membranes is also likely to be distinctive but the involvement of specific lipids in H_2O_2 membrane transfer remains to be addressed.

We hypothesized that the H_2O_2 transient would modulate Ca^{2+} release, and isolated the effect by artificially producing ROS at the interface in the absence of Ca^{2+} elevation. This experiment confirmed that ROS specific to the interface sensitized cells to agonist-induced Ca^{2+}-release and that H_2O_2 acts locally since ROS production at the distant nucleus was without effect. We suggest that the H_2O_2 transient regulates the IP_3 receptor via the oxidation of specific thiol groups (Bansaghi et al., 2014). When the H_2O_2 transient was prevented, Ca^{2+} oscillations were inhibited, implying that a Ca^{2+}-release event makes subsequent events more likely using mitochondrial H_2O_2 as a feed-forward sensitizing agent. However, this does not produce a vicious cycle, since the cristae pool is finite. Instead, the interface will not be oxidized by subsequent Ca^{2+} elevations until mitochondria have "reset" their matrix volume. In this way, mitochondria may protect themselves against Ca^{2+} overload during IP_3-linked $[Ca^{2+}]_c$ oscillations. Conversely, "rested" mitochondria signal their readiness to accept further Ca^{2+}. We predict that mitochondria can regulate both IP_3 and ryanodine receptor-mediated $[Ca^{2+}]_c$ oscillations via ROS nanodomains since

ryanodine receptors also transfer Ca^{2+} locally to the mitochondria (Pacher et al., 2002) and display H_2O_2-mediated sensitization (Favero et al., 1995).

Links between Ca^{2+}/K^+ matrix volume and mitochondrial metabolism were made long ago (Halestrap, 1994), but changes in the cristae/IMS volume were not addressed. That this volume may be physically exchanged with the interface implies that all solutes enriched or depleted by ETC activity, such as ATP, are exchanged. Our data show that the ER-mitochondrial interface hosts concentrations of signaling molecules which are extreme compared to those found in the bulk cytosol. Such concentrations deliver excellent signal-to-noise ratio, but are confined to prevent the consequences of Ca^{2+} or H_2O_2 overload in the whole cell. Our model constitutes a new mechanism by which mitochondrial metabolism and the intensity and shape of Ca^{2+} signals are linked and controlled. These mechanisms regulate and initiate diverse processes. Conversely, deregulation of this system may be a crucial component of subcellular pathology.

Experimental Procedures

Targeting of proteins to the ER-mitochondial interface

The selective targeting of proteins to the ER-mitochondial interface was achieved by targeting one half of the rapamycin binding protein heterodimers (FKBP12) to the cytosolic surface of the OMM with the N-terminal sequence of the mAKAP1 (34–63). The two were joined by fusion proteins tagged with mRFP, HyPer (Belousov et al., 2006), SypHer (Poburko et al., 2011) or Killer Red (Bulina et al., 2006) in the pEGFP-N1 plasmid backbone. The constructs used for targeting the mRFP-tagged FRB protein to the cytoplasmic surface of the ER were described elsewhere (Varnai and Balla, 2007) and were adapted by replacing mRFP with HyPer, SypHer or Killer Red. Proteins were concentrated/trapped at the ER-mitochondrial interface by the induction of heterodimerization using rapamycin (100 nM, 3–5 mins). Dimerization was halted by blocking FKBP with FK506 (1 μM).

Live cell imaging

For imaging experiments, HepG2 cells were pre-incubated in a serum-free extracellular medium (ECM, 121 mM NaCl, 5 mM $NaHCO_3$, 10 mM Na-HEPES, 4.7 mM KCl, 1.2 mM KH_2PO4, 1.2 mM $MgSO_4$, 2 mM $CaCl_2$, 10 mM glucose, pH7.4) containing 2% BSA. For measurements of $[Ca^{2+}]_c$, cells were loaded with fura2-AM together with 0.003% pluronic F127 and 100 μM sulfinpyrazone for 30 min at room temperature. At the end of the preincubation or dye-loading period the cells were washed into a fresh ECM containing 0.25% BSA and transferred to the temperature-regulated stage (37°C) of the microscope.

Fluorescence wide-field imaging of H_2O_2, pH, $[Ca^{2+}]_c$, and $[Ca^{2+}]_m$ was carried out using a back-illuminated EMCCD camera (Photometrics). HyPer/SypHer were imaged with 495/20 nm and 415/30 nm excitation filters and a 500 nm long-pass beam splitter, and an image pair was obtained every 2.5 s to minimize photodamage. Fluorescence is presented as 495/415 nm ratios calculated following background subtraction of the individual wavelengths. $[Ca^{2+}]_c$ measured with fura2 in intact cells (excitation 340/30 nm, 380/20 nm) was

calibrated as described (Csordas et al., 2006). $[Ca^{2+}]_m$ was measured simultaneously with $[Ca^{2+}]_c$ using RCaMP (excitation 545/20 nm, dual-band dichroic and emission: 73100, Chroma) image series were collected every 1.0 s for accurate kinetic information and data was expressed as $F/F_0 \pm$ SEM.

Confocal imaging was carried out using a Zeiss LSM 780 system using 405, 488 and 561 nm lines for cyan, green and red fluorescent probes, respectively. High-resolution images were taken using a 60× oil objective (NA 1.40). Contrast and brightness were optimized in the brightest slice of the stack, and the same settings were applied to the rest of the sections. Co-localization image acquisition and analysis using Zen 2010 (Carl Zeiss, Jena) were performed to calculate changes in Pearson's coefficients (R^2).

Transmission electron microscopy

HepG2 cells grown in T25 flasks were preincubated in 2% BSA-ECM (60 min, 37°C), and subsequently, were pre-treated with paxilline (25 μM) or valinomycin (0.5 nM) followed by stimulation with agonist (ATP, 100 μM) in 0.25% BSA-containing ECM for 1min. Samples were fixed, processed and visualized as described before (Pacher et al., 2000). Image analysis was as described (Csordas et al., 2006). Measurements of mitochondrial cross sectional area were made of sections containing complete and partial mitochondria. Measurements are therefore a likely underestimate of actual mitochondrial size. Tomogram was obtained from a tilt series. A 150 nm section was imaged through 116° at one image per degree. The tomogram was aligned and reconstructed using FEI Inspect3d software and visualized using Amira.

A full description of the experimental procedures is within the supplementary material.

Supplementary Material

Refer to Web version on PubMed Central for supplementary material.

Acknowledgments

We thank György Csordás and David Weaver for help with electron microscopy and tomography. This work was supported by NIH grants GM59419 and ES025672 to G.H., Hungarian Scientific Research Fund OTKA K105006 to P.V. and K106138 to M.G. and a 'Momentum' grant from the Hungarian Academy of Sciences to M.G..

References

Aon MA, Cortassa S, Marban E, O'Rourke B. Synchronized whole cell oscillations in mitochondrial metabolism triggered by a local release of reactive oxygen species in cardiac myocytes. The Journal of biological chemistry. 2003; 278:44735–44744. [PubMed: 12930841]

Araki K, Iemura S, Kamiya Y, Ron D, Kato K, Natsume T, Nagata K. Ero1-alpha and PDIs constitute a hierarchical electron transfer network of endoplasmic reticulum oxidoreductases. The Journal of cell biology. 2013; 202:861–874. [PubMed: 24043701]

Bader M, Muse W, Ballou DP, Gassner C, Bardwell JC. Oxidative protein folding is driven by the electron transport system. Cell. 1999; 98:217–227. [PubMed: 10428033]

Bansaghi S, Golenar T, Madesh M, Csordas G, Ramachandrarao S, Sharma K, Yule DI, Joseph SK, Hajnoczky G. Isoform- and Species-specific Control of Inositol 1,4,5-Trisphosphate (IP3) Receptors by Reactive Oxygen Species. The Journal of biological chemistry. 2014; 289:8170–8181. [PubMed: 24469450]

Belousov VV, Fradkov AF, Lukyanov KA, Staroverov DB, Shakhbazov KS, Terskikh AV, Lukyanov S. Genetically encoded fluorescent indicator for intracellular hydrogen peroxide. Nature methods. 2006; 3:281–286. [PubMed: 16554833]

Bilan DS, Belousov VV. HyPer Family Probes: State of the Art. Antioxidants & redox signaling. 2016

Bootman MD, Taylor CW, Berridge MJ. The thiol reagent, thimerosal, evokes Ca2+ spikes in HeLa cells by sensitizing the inositol 1,4,5-trisphosphate receptor. The Journal of biological chemistry. 1992; 267:25113–25119. [PubMed: 1334081]

Bulina ME, Chudakov DM, Britanova OV, Yanushevich YG, Staroverov DB, Chepurnykh TV, Merzlyak EM, Shkrob MA, Lukyanov S, Lukyanov KA. A genetically encoded photosensitizer. Nature biotechnology. 2006; 24:95–99.

Cogliati S, Frezza C, Soriano ME, Varanita T, Quintana-Cabrera R, Corrado M, Cipolat S, Costa V, Casarin A, Gomes LC, et al. Mitochondrial cristae shape determines respiratory chain supercomplexes assembly and respiratory efficiency. Cell. 2013; 155:160–171. [PubMed: 24055366]

Csordas G, Hajnoczky G. SR/ER-mitochondrial local communication: calcium and ROS. Biochimica et biophysica acta. 2009; 1787:1352–1362. [PubMed: 19527680]

Csordas G, Renken C, Varnai P, Walter L, Weaver D, Buttle KF, Balla T, Mannella CA, Hajnoczky G. Structural and functional features and significance of the physical linkage between ER and mitochondria. The Journal of cell biology. 2006; 174:915–921. [PubMed: 16982799]

Csordas G, Thomas AP, Hajnoczky G. Quasi-synaptic calcium signal transmission between endoplasmic reticulum and mitochondria. The EMBO journal. 1999; 18:96–108. [PubMed: 9878054]

Csordas G, Varnai P, Golenar T, Roy S, Purkins G, Schneider TG, Balla T, Hajnoczky G. Imaging interorganelle contacts and local calcium dynamics at the ER-mitochondrial interface. Molecular cell. 2010; 39:121–132. [PubMed: 20603080]

Dickinson DA, Forman HJ. Cellular glutathione and thiols metabolism. Biochemical pharmacology. 2002; 64:1019–1026. [PubMed: 12213601]

Duchen MR. Ca(2+)-dependent changes in the mitochondrial energetics in single dissociated mouse sensory neurons. The Biochemical journal. 1992; 283(Pt 1):41–50. [PubMed: 1373604]

Favero TG, Zable AC, Abramson JJ. Hydrogen peroxide stimulates the Ca2+ release channel from skeletal muscle sarcoplasmic reticulum. The Journal of biological chemistry. 1995; 270:25557–25563. [PubMed: 7592726]

Giacomello M, Drago I, Bortolozzi M, Scorzeto M, Gianelle A, Pizzo P, Pozzan T. Ca2+ hot spots on the mitochondrial surface are generated by Ca2+ mobilization from stores, but not by activation of store-operated Ca2+ channels. Molecular cell. 2010; 38:280–290. [PubMed: 20417605]

Halestrap AP. Regulation of mitochondrial metabolism through changes in matrix volume. Biochemical Society transactions. 1994; 22:522–529. [PubMed: 7958359]

Halestrap AP, Quinlan PT, Whipps DE, Armston AE. Regulation of the mitochondrial matrix volume in vivo and in vitro. The role of calcium. The Biochemical journal. 1986; 236:779–787. [PubMed: 2431681]

Jouaville LS, Pinton P, Bastianutto C, Rutter GA, Rizzuto R. Regulation of mitochondrial ATP synthesis by calcium: evidence for a long-term metabolic priming. Proceedings of the National Academy of Sciences of the United States of America. 1999; 96:13807–13812. [PubMed: 10570154]

Kirichok Y, Krapivinsky G, Clapham DE. The mitochondrial calcium uniporter is a highly selective ion channel. Nature. 2004; 427:360–364. [PubMed: 14737170]

Li G, Mongillo M, Chin KT, Harding H, Ron D, Marks AR, Tabas I. Role of ERO1-alpha-mediated stimulation of inositol 1,4,5-triphosphate receptor activity in endoplasmic reticulum stress-induced apoptosis. The Journal of cell biology. 2009; 186:783–792. [PubMed: 19752026]

Liu X, Hajnoczky G. Altered fusion dynamics underlie unique morphological changes in mitochondria during hypoxia-reoxygenation stress. Cell death and differentiation. 2011; 18:1561–1572. [PubMed: 21372848]

Marchissio MJ, Frances DE, Carnovale CE, Marinelli RA. Mitochondrial aquaporin-8 knockdown in human hepatoma HepG2 cells causes ROS-induced mitochondrial depolarization and loss of viability. Toxicology and applied pharmacology. 2012; 264:246–254. [PubMed: 22910329]

Pacher P, Csordas P, Schneider T, Hajnoczky G. Quantification of calcium signal transmission from sarco-endoplasmic reticulum to the mitochondria. The Journal of physiology. 2000; 529(Pt 3): 553–564. [PubMed: 11118489]

Pacher P, Thomas AP, Hajnoczky G. Ca2+ marks: miniature calcium signals in single mitochondria driven by ryanodine receptors. Proceedings of the National Academy of Sciences of the United States of America. 2002; 99:2380–2385. [PubMed: 11854531]

Picard M, McManus MJ, Csordas G, Varnai P, Dorn GW 2nd, Williams D, Hajnoczky G, Wallace DC. Trans-mitochondrial coordination of cristae at regulated membrane junctions. Nature communications. 2015; 6:6259.

Poburko D, Santo-Domingo J, Demaurex N. Dynamic regulation of the mitochondrial proton gradient during cytosolic calcium elevations. The Journal of biological chemistry. 2011; 286:11672–11684. [PubMed: 21224385]

Prosser BL, Ward CW, Lederer WJ. X-ROS signaling: rapid mechano-chemo transduction in heart. Science. 2011; 333:1440–1445. [PubMed: 21903813]

Quinlan PT, Thomas AP, Armston AE, Halestrap AP. Measurement of the intramitochondrial volume in hepatocytes without cell disruption and its elevation by hormones and valinomycin. The Biochemical journal. 1983; 214:395–404. [PubMed: 6412700]

Rizzuto R, Brini M, Murgia M, Pozzan T. Microdomains with high Ca2+ close to IP3-sensitive channels that are sensed by neighboring mitochondria. Science. 1993; 262:744–747. [PubMed: 8235595]

Rizzuto R, Pinton P, Carrington W, Fay FS, Fogarty KE, Lifshitz LM, Tuft RA, Pozzan T. Close contacts with the endoplasmic reticulum as determinants of mitochondrial Ca2+ responses. Science. 1998; 280:1763–1766. [PubMed: 9624056]

Sena LA, Chandel NS. Physiological roles of mitochondrial reactive oxygen species. Molecular cell. 2012; 48:158–167. [PubMed: 23102266]

Singh H, Lu R, Bopassa JC, Meredith AL, Stefani E, Toro L. MitoBK(Ca) is encoded by the Kcnma1 gene, and a splicing sequence defines its mitochondrial location. Proceedings of the National Academy of Sciences of the United States of America. 2013; 110:10836–10841. [PubMed: 23754429]

Szabadkai G, Bianchi K, Varnai P, De Stefani D, Wieckowski MR, Cavagna D, Nagy AI, Balla T, Rizzuto R. Chaperone-mediated coupling of endoplasmic reticulum and mitochondrial Ca2+ channels. The Journal of cell biology. 2006; 175:901–911. [PubMed: 17178908]

Szalai G, Krishnamurthy R, Hajnoczky G. Apoptosis driven by IP(3)-linked mitochondrial calcium signals. The EMBO journal. 1999; 18:6349–6361. [PubMed: 10562547]

Umanskaya A, Santulli G, Xie W, Andersson DC, Reiken SR, Marks AR. Genetically enhancing mitochondrial antioxidant activity improves muscle function in aging. Proceedings of the National Academy of Sciences of the United States of America. 2014; 111:15250–15255. [PubMed: 25288763]

Varnai P, Balla T. Visualization and manipulation of phosphoinositide dynamics in live cells using engineered protein domains. Pflugers Archiv : European journal of physiology. 2007; 455:69–82. [PubMed: 17473931]

Wang W, Fang H, Groom L, Cheng A, Zhang W, Liu J, Wang X, Li K, Han P, Zheng M, et al. Superoxide flashes in single mitochondria. Cell. 2008; 134:279–290. [PubMed: 18662543]

Xu W, Liu Y, Wang S, McDonald T, Van Eyk JE, Sidor A, O'Rourke B. Cytoprotective role of Ca2+-activated K+ channels in the cardiac inner mitochondrial membrane. Science. 2002; 298:1029–1033. [PubMed: 12411707]

Zhao R, Masayasu H, Holmgren A. Ebselen: a substrate for human thioredoxin reductase strongly stimulating its hydroperoxide reductase activity and a superfast thioredoxin oxidant. Proceedings of the National Academy of Sciences of the United States of America. 2002; 99:8579–8584. [PubMed: 12070343]

Zhao Y, Wang ZB, Xu JX. Effect of cytochrome c on the generation and elimination of O2*- and H2O2 in mitochondria. The Journal of biological chemistry. 2003; 278:2356–2360. [PubMed: 12435729]

Zorov DB, Filburn CR, Klotz LO, Zweier JL, Sollott SJ. Reactive oxygen species (ROS)-induced ROS release: a new phenomenon accompanying induction of the mitochondrial permeability transition in cardiac myocytes. J Exp Med. 2000; 192:1001–1014. [PubMed: 11015441]

Highlights

- The ER-mitochondrial interface hosts a dynamic H_2O_2 nanodomain.
- ER-mitochondrial Ca^{2+} transfer stimulates ROS mobilization from mitochondria.
- The oxidized cristae volume is the source of interface H_2O_2 transients.
- H_2O_2 transients sensitize ER Ca^{2+}-release to maintain Ca^{2+} oscillations.

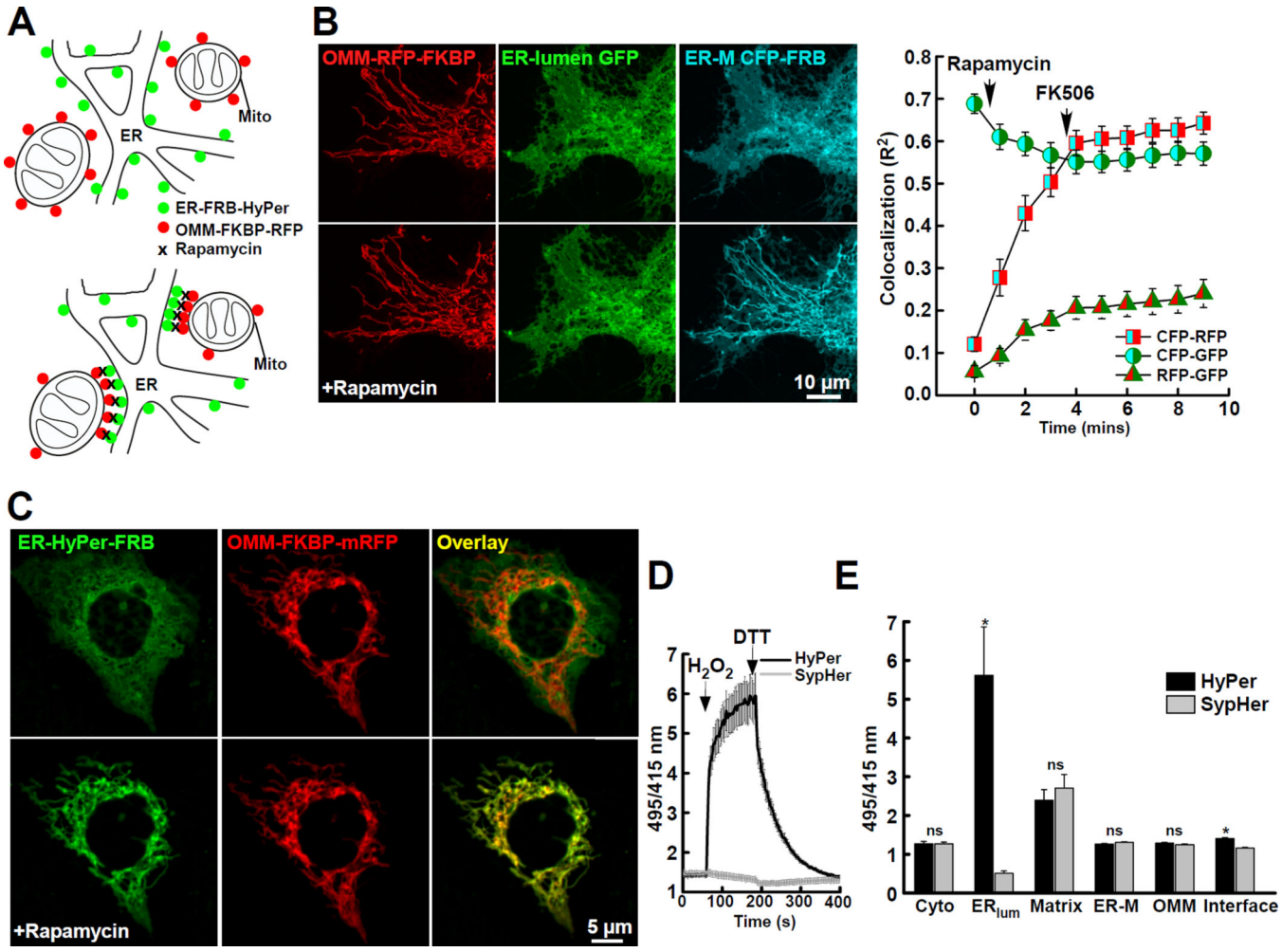

Fig. 1. Measurement of H_2O_2 Nanodomains with Inducible Targeting

(A) Scheme depicting the targeting of fluorescent proteins to the surface of the endoplasmic reticulum (ER-M; green) and the OMM (red) with FRB and FKBP linker halves linked to the targeting sequences sac1(521–587) and mAKAP1(34–63), respectively (upper). Rapamycin-induced heterodimerization of linker halves causes concentration of the dimers at the ER-mitochondrial interface (lower). For further details see (Csordas et al., 2010).

(B) Images of HepG2 cells and co-localization analysis showing that heterodimerization of linker halves progressively changes the distribution of the ER-surface targeted probe (ER-M CFP-FRB; cyan) to co-localize (right; CFP-RFP, squares) with OMM targeted probes (OMM-mRFP-FKBP; red) and separate from ER-lumen targeted GFP (ER-lumen GFP; green) in response to rapamycin (ER-M CFP-FRB; cyan, lower). Further changes in probe distribution are blocked by rapamycin removal and addition of FK506 (5 µM). The overall ER structure (green) remains essentially unchanged by rapamycin treatment.

(C) Distribution of ER-surface H_2O_2-sensor HyPer (ER-HyPer-FRB; green) before and after heterodimerization with OMM-mRFP–FKBP (red). Images collected before (upper) and after rapamycin (100 nM for 5min; lower).

(D) Response of interface-targeted HyPer (black) and H_2O_2 insensitive derivative SypHer (gray), to H_2O_2 (200 µM) and dithiothreitol (DTT; 5 mM) (mean±SEM, n = 48 cells).

(E) Measurements using HyPer and SypHer targeted to the cytosol, ER lumen, mitochondrial matrix, cytosolic surface of the ER (ER-M) and OMM. (* = $p < 0.05$; n = 3 experiments >50 cells/condition).
See also Figure S1.

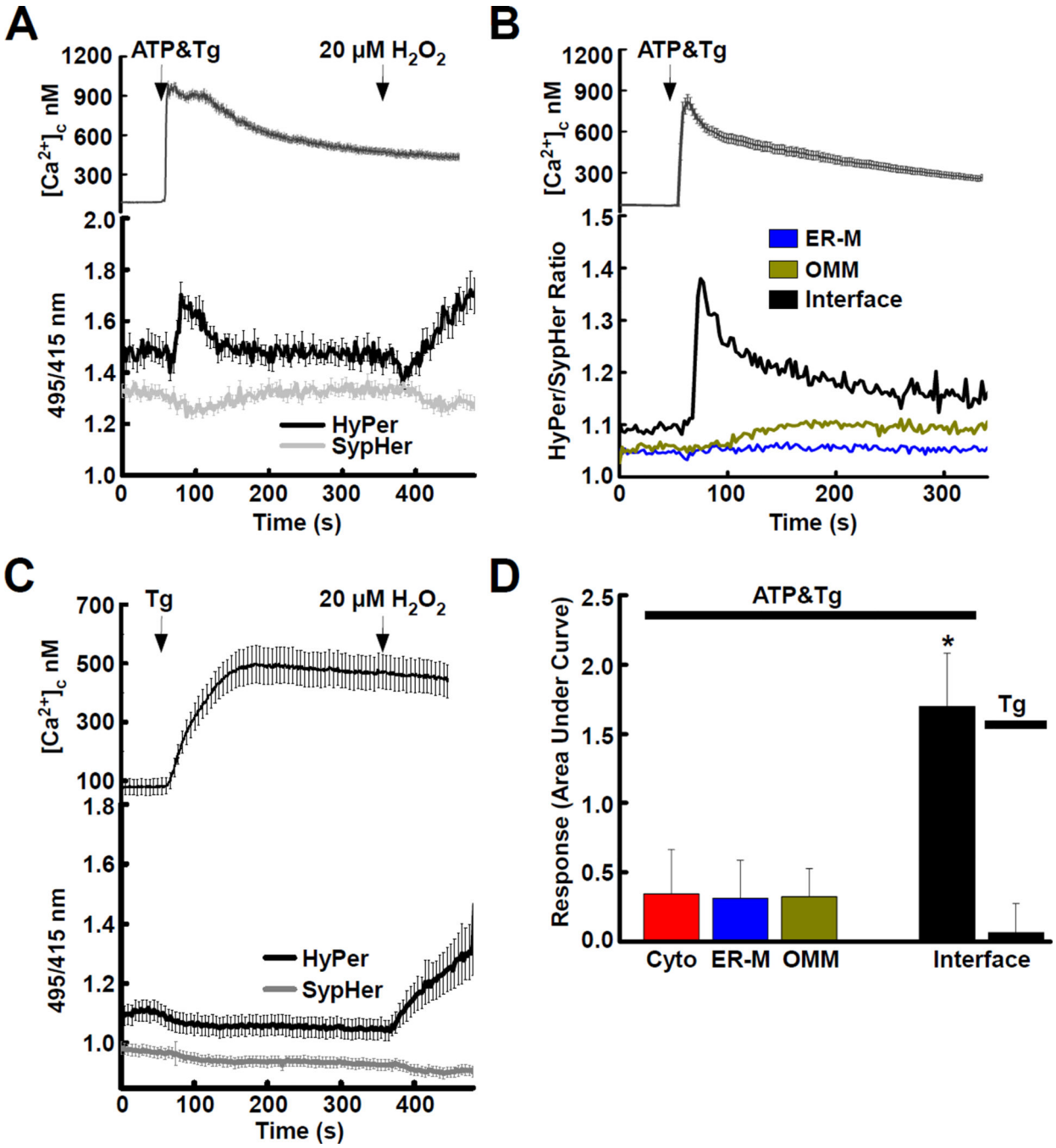

Fig. 2. ER-mitochondrial H_2O_2 nanodomains are induced by agonist stimulation

(A) Global $[Ca^{2+}]_c$ rise (top) and ratio changes of interface-targeted HyPer (*black*) and SypHer (*gray*) (bottom) evoked by simultaneous stimulation with an IP_3-linked agonist, (ATP, 100 μM) and the SERCA pump inhibitor, thapsigargin (Tg, 2 μM) are shown (mean ±SEM). H_2O_2 is added as a positive control (20 μM). Both HyPer and SypHer respond to pH changes that accompany $[Ca^{2+}]_c$ signals: changes common to both probes are attributable to pH, changes seen in HyPer only are caused by H_2O_2. Based on the study of Poburko et al. (Poburko et al., 2011) and our results we conclude that an acidification

followed by an alkalization occurred during stimulation. Such changes underscore the need for parallel fluorescence recordings using HyPer and SypHer when one wants to measure H_2O_2.

(B) (top) $[Ca^{2+}]_c$ rise and (bottom) mean HyPer/SypHer ratios of probes concentrated at the interface (black, n = 59) or diffused along the entire OMM (*yellow*, n = 41) or ER-M (*blue*, n = 41). (C) (top) Global $[Ca^{2+}]_c$ rise and (bottom) HyPer (*black*) and SypHer (*gray*) ratio changes evoked by stimulation with Tg (2 μM) alone, shown (mean±SEM).

(D) Quantitation of H_2O_2 increase as the area under curve (AUC) $((\text{HyPer/SypHer} \times \text{time})_{response} - (\text{HyPer/SypHer} \times \text{time})_{baseline}$; * p = < 0.05). From cells treated with ATP&Tg or Tg alone.

See also Figure S2.

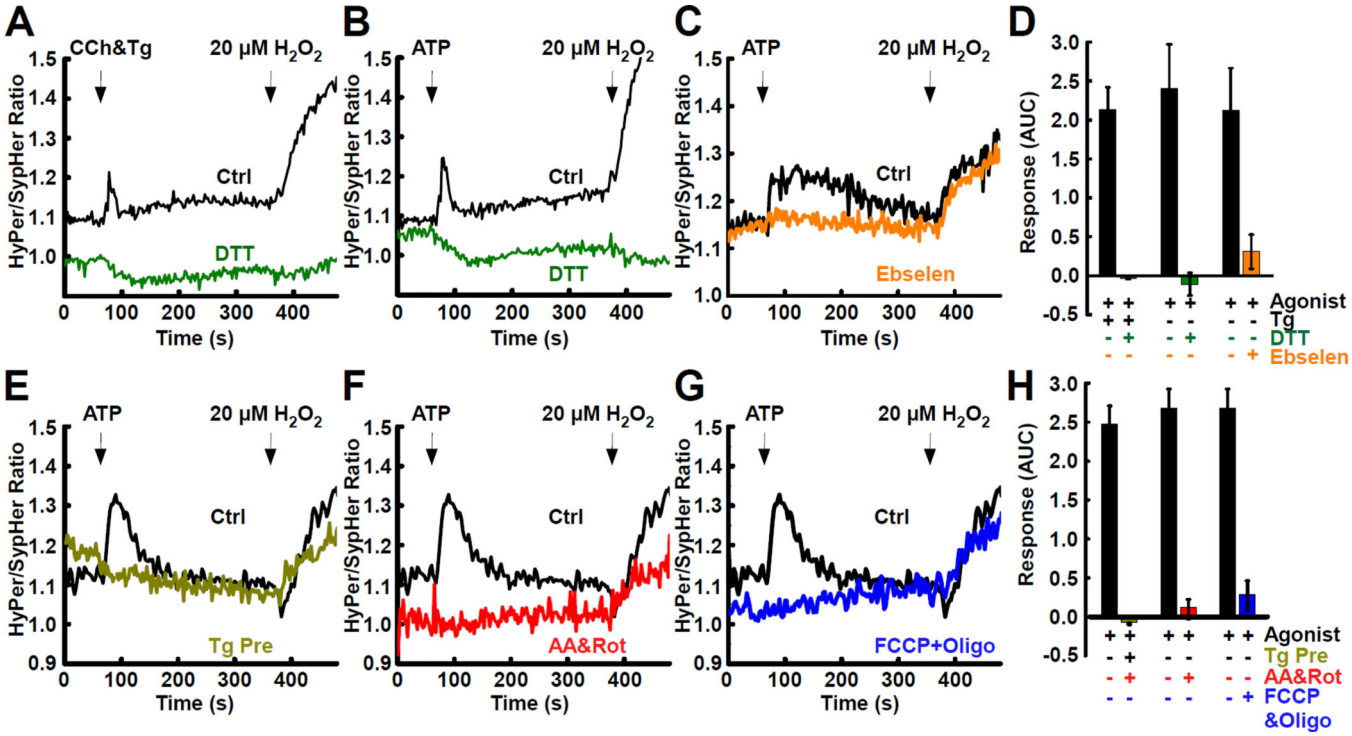

Fig. 3. IP_3 Receptor-mediated ER Ca^{2+} Mobilization and Mitochondrial Respiratory Chain Cunction are Required for the Generation of H_2O_2 Nanodomains

HepG2 cells expressing ER-M HyPer and OMM HyPer or ER-M SypHer and OMM SypHer were all subjected to a pulse of rapamycin (100 nM, 5 mins) and an FK506 wash (5 μM) to target the probes to the ER-mitochondrial interface. Traces are presented as HyPer/SypHer ratios. (A) Carbachol (CCh, 100 μM) plus thapsigargin (Tg, 2 μM) or (B) ATP (100 μM) alone, in control cells (*black*, n = 108 and 78, respectively) and DTT pre-treated cells (5 mM, *green*, n = 44 and 50, respectively) on the time course of interface-targeted HyPer/SypHer ratios.

(C) Pre-incubation with Gpx analog Ebselen (25 μM; orange, n = 68) abolishes agonist-induced response (black, *n* = 231).

(D) Area under curve (AUC) quantification of interface H_2O_2 in response to agonist ±Tg, DTT and ebselen. Prevention of the interface H_2O_2 nanodomains by (E) discharge of ER Ca^{2+} using 0 Ca^{2+} extracellular medium supplemented with Tg (2 μM) (*yellow*, n = 87), (F) antimycin A (5 μM) and rotenone (5 μM 10 mins; *red*, n = 121) or (G) FCCP (5 μM) and oligomycin (10 μM; *blue*, n = 133). All were compared to control (*black*, n = 132).

(G) AUC quantification of interface H_2O_2 following pre-treatment with 0 Ca^{2+} & Tg (*yellow*), antimycin A & rotenone (*red*) and FCCP & oligomycin (*blue*).

See also Figure S3.

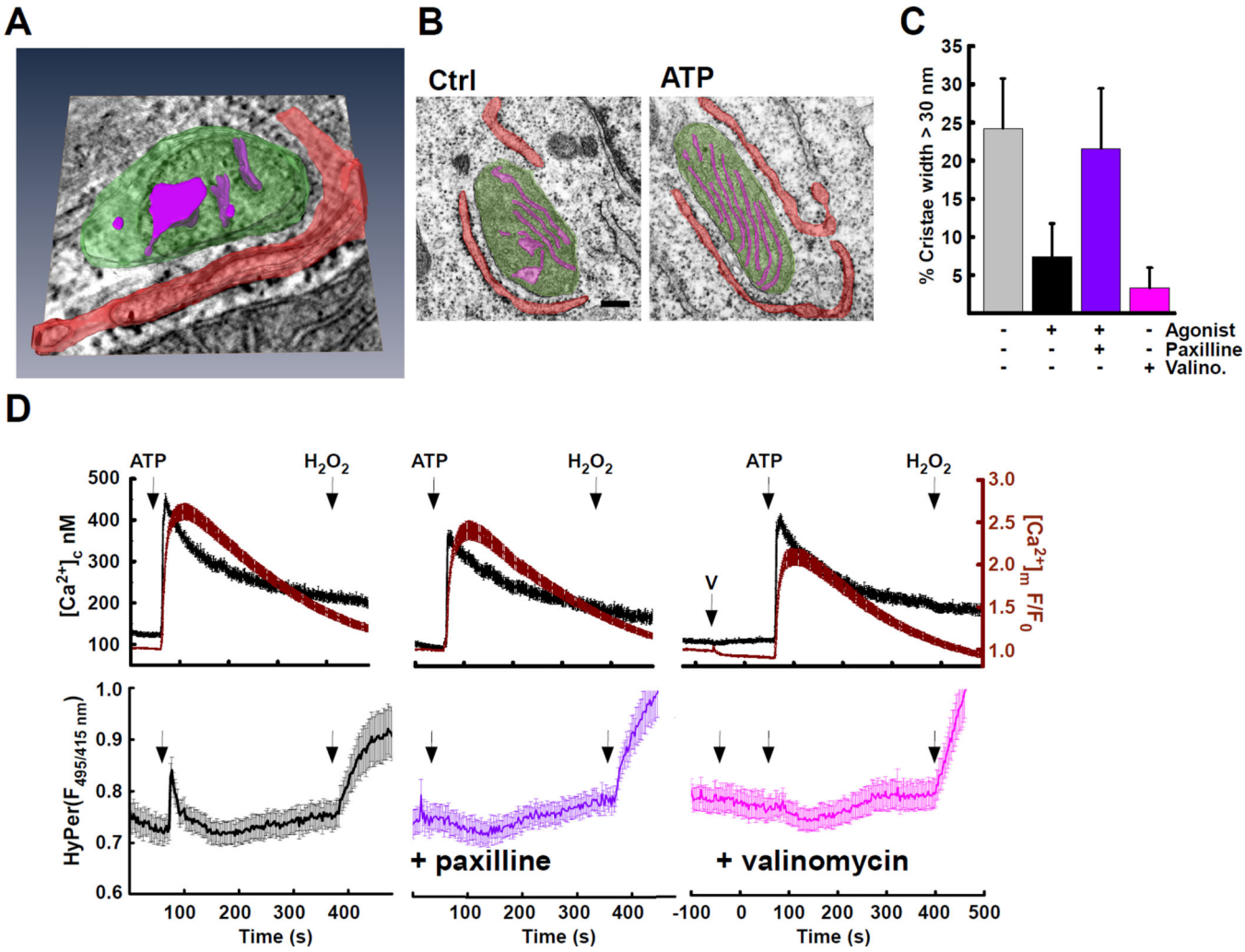

Fig. 4. Matrix and Cristae Volume Changes in Response to Agonist Stimulation

(A) Electron tomography of a HepG2 cell. Mitochondrial volume (*green*), cristae (*magenta*) and ER (*red*). Both dilated and collapsed cristae are shown. Note orientation of several cristae openings to the ER-mitochondrial interface. Representative of 7 datasets.

(B) Transmission electron microscopy images of single HepG2 mitochondria false colored to highlight ER (red) mitochondrial matrix (*green*) and cristae (*magenta*) ± ATP stimulation (100 μM for 1 min). The scale bar is 100 nm.

(C) Frequency of wide cristae (>30 nm) were measured in control (*gray*) and ATP-stimulated conditions (*black*). Agonist stimulation was applied to cells pre-incubated with an inhibitor of mitoBK$_{Ca}$ (paxilline 25μM; *purple*) or treated with a non-depolarizing concentration of the K$^+$-ionophore (valinomycin 0.5 nM; *pink*) alone. Ctrl vs ATP and Ctrl vs Valino are p = < 0.05, ANOVA.

(D) (top) [Ca^{2+}]$_c$ (*black*), was measured simultaneously with [Ca^{2+}]$_m$ (*dark red*). (bottom) In parallel, measurements were made with interface-targeted HyPer (mean±SEM). Cells were stimulated with agonist (ATP; 100 μM) in control conditions (*black*, n = 116) after pre-treatment with mitoBKCa inhibitor (paxilline; 25μM, *purple*, n = 98) after K$^+$ ionophore

("V" valinomycin; 0.5 nM, 60 s, *pink*, n = 91). H_2O_2 is added at the end of the experiment as a positive control (20 μM).
See also Figure S4.

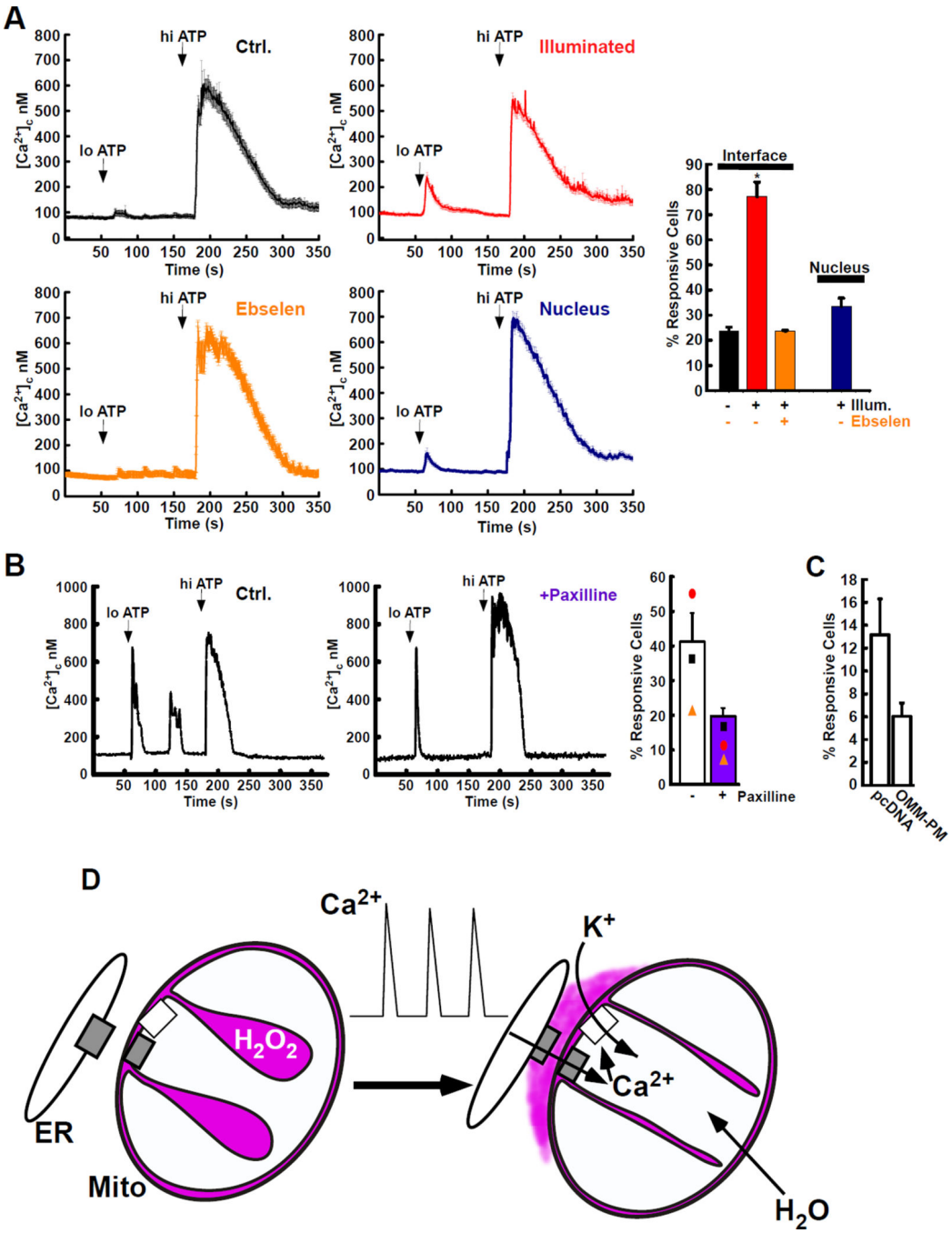

Fig. 5. Cristae-derived ROS modulates Ca^{2+}-release

(A) Cells expressing Killer Red (KR) targeted to the interface with drug-inducible linker (*black, red* & *orange*; mean±SEM) or to the nucleus (*blue*) were stage-incubated in the dark (300 s, Ctrl, *black*) or with green light (545/25 nm, 300 s, *red, orange* and *blue*) to induce KR-derrived ROS. $[Ca^{2+}]_c$ was assessed in response to stepwise increase in IP_3-linked agonist concentration (loATP, 1 μM; hiATP, 100 μM) in the absence of external Ca^{2+}. Cells were assessed for response to loATP, after illumination and pre-incubation with the ebselen (25 μM, *orange*). Responses to loATP were quantified (right panel, % response loATP; Ctrl,

black, n = 61; Illuminated, *red*, n = 64). Ebselen, (*orange*, n = 62). Nucleus, (*blue*, n = 122) (* p = < 0.05).

(B) Sample traces of cells assessed for repetitive $[Ca^{2+}]_c$ spiking without treatment (Ctrl., left) or pre-incubated with mitoBK$_{Ca}$ inhibitor (paxilline, 25 μM, center). Quantification of responsive cells ($[Ca^{2+}]_c$ spikes ≥ 1 following loATP) demonstrating repetitive (>1) $[Ca^{2+}]_c$ spikes in response to loATP, (right, Mean±SEM and means of individual experiments).

(C) Percent of cells showing $[Ca^{2+}]_c$ response to loATP when transfected with pcDNA (n = 106) or a constitutive OMM-plasma membrane linker (AKAP-RFP-CAAX, n = 94).

(D) Scheme of hypothesis; IMS and cristae volume (purple), Ca^{2+} transport proteins (gray) and mitoBK^{Ca} (white). ER Ca^{2+} release events (center) increase matrix Ca^{2+}, activate K^+-uptake and increase matrix volume. H_2O_2-rich cristae volume is forced to the ER-mitochondrial interface.